Published in final edited form as:

Oncogene. 2010 February 11; 29(6): 789–801. doi:10.1038/onc.2009.383.

Anthrax Toxin Receptor 2 is expressed in murine and tumor vasculature and functions in endothelial proliferation and morphogenesis

Claire V. Reeves[*,†], **Joseph Dufraine**[*,†], **John A. T. Young**[§], and **Jan Kitajewski**[*,†,‡]

[*] OB/GYN, Columbia University Medical Center, New York, NY 10032 USA

[†] Pathology, Columbia University Medical Center, New York, NY 10032 USA

[‡] Herbert Irving Comprehensive Cancer Center, Columbia University Medical Center, New York, NY 10032 USA

[§] Infectious Disease Laboratory, The Salk Institute for Biological Studies, La Jolla, CA 92037 USA

Abstract

The Capillary Morphogenesis Gene 2 (CMG2) gene encodes an Anthrax toxin receptor (ANTXR2) but the normal physiological function is not known. *ANTXR2/CMG2* was originally identified as a result of up-regulation during capillary morphogenesis of endothelial cells cultured *in vitro*. We explored the hypothesis that key steps of the angiogenic process are either dependent or are influenced by ANTXR2/CMG2 activity. We describe the expression pattern of ANTXR2/CMG2 in several murine tissues and in normal breast and breast tumors. Endothelial expression was found in all of the tissues analyzed, in cultured endothelial cells and in breast tumor vessels; however ANTXR2/CMG2 expression was not restricted to this cell type. To assess potential angiogenic function, we utilized RNA interference to achieve significant reduction of ANTXR2/CMG2 expression in cultured human umbilical venous endothelial cells. Reduced ANTXR2/CMG2 expression resulted in significant inhibition of proliferation and reduced capacity of endothelial cells to form capillary-like networks *in vitro*, while overexpression of ANTXR2/CMG2 in HUVEC increased proliferation and capillary-like network formation. Little change in migration of endothelial cells was observed upon knockdown or overexpression. We conclude that ANTXR2/CMG2 functions to promote endothelial proliferation and morphogenesis during sprouting angiogenesis, consistent with the endothelial expression of ANTXR2/CMG2 in several vascular beds.

Keywords

ANTXR2; CMG2; angiogenesis; endothelial cells

Please address proofs to Dr. Jan Kitajewski: 1130 Saint Nicholas Avenue, Irving Cancer Research Center, Office 926, Columbia University, New York, NY 10035, contact telephone number: 212-851-4688, contact fax number: 212-851-4504, jkk9@columbia.edu.

Highest Degree Obtained: Claire V. Reeves, Master of Philosophy; Joseph Dufraine, Master of Philosophy; John A. T. Young, Doctor of Philosophy; Jan Kitajewski, Doctor of Philosophy.

Introduction

Angiogenesis, the process by which new blood vessels are derived from pre-existing vessels, is essential for physiological processes such as embryonic development, female reproduction, wound healing and pathological processes such as tumor growth, atherosclerosis and diabetic retinopathy (Carmeliet and Jain, 2000). The mechanism of angiogenesis is often divided into distinct cellular phases in order to facilitate the study of this complex process. During the initial phase, endothelial cells (ECs) are stimulated to degrade and invade the underlying basement membrane and interstitial matrix. The cells then proliferate and migrate to form cordlike structures. Finally, differentiation occurs in which vessel lumens are formed, new basement membranes are produced, and accessory cells are recruited to stabilize new vessels, reviewed in (Adams and Alitalo, 2007; Armulik *et al.*, 2005; Risau, 1997). An understanding at the molecular level as to how ECs assemble into new vessels is not fully understood, but depends on several angiogenic signaling pathways derived from cell surface receptors, such as the VEGF Receptors. *In vitro* assays designed to model the distinct steps of angiogenesis have proven useful in elucidating potential angiogenic regulators. For example, genes involved in capillary morphogenesis have been discovered using an EC morphogenesis assay in which ECs are suspended as individual cells in 3D collagen matrices (Bell *et al.*, 2001). Capillary Morphogenesis Gene 2 (CMG2) was originally identified in this manner. *CMG2* was demonstrated to be a gene with dramatically up-regulated expression in cultured human umbilical venous endothelial cells (HUVEC) induced to undergo capillary morphogenesis *in vitro* (Bell *et al.*, 2001). The gene is predicted to express four different proteins from alternatively spliced mRNAs; including $CMG2^{489}$, $CMG2^{488}$, $CMG2^{386}$ and $CMG2^{322}$ transcripts (Scobie *et al.*, 2003). $CMG2^{489}$ and $CMG2^{488}$ are thought to reside at the cell surface as they contain signal sequences and are type I membrane proteins, but they differ as $CMG2^{488}$ has an alternate 13 amino acids at the C-terminus. These two isoforms contain an extracellular region with a von Willebrand factor type A (vWF) domain, a transmembrane domain and a cytosolic tail of unknown function. The vWF domain contains a metal ion-dependent adhesion site (MIDAS) consisting of five amino acid residues (DXSXS…T…D; where X can be any amino acid) that chelates a divalent cation critical for ligand binding (Shimaoka *et al.*, 2002). vWF domains are known to facilitate protein-protein interactions when found on extracellular matrix constituents or cell adhesion proteins like α-integrin subunits and are thought to constitute ligand binding sites on CMG2. $CMG2^{386}$ is also a transmembrane protein, but it has been demonstrated to reside at the endoplasmic reticulum membrane (Bell *et al.*, 2001). It is identical in amino acid composition to $CMG2^{489}$ except that it lacks 100 amino acids between the vWF domain and the transmembrane domain. $CMG2^{322}$ is predicted to contain a signal peptide and vWF domain identical to $CMG2^{489}$, but since $CMG2^{322}$ lacks a transmembrane domain this protein is predicted to undergo secretion.

Physiological receptor activity for CMG2 remains unknown given that there are no immediately recognizable signaling domains in the cytosolic tails. However, it is known that mutations in the *CMG2* gene result in the human autosomal recessive syndromes, juvenile hyaline fibromatosis and infantile systemic hyalinosis (Hanks *et al.*, 2003). These syndromes are characterized by recurrent subcutaneous tumors, gingival hypertrophy, joint

contractures, osteolysis, osteoporosis, and hyaline depositions. The cellular basis of these related diseases and the degree of CMG2 loss of function due to mutations in affected individuals are currently not well understood. Finally, independent of the discovery of the gene being expressed during capillary morphogenesis and its association with a human disease, *CMG2* has been revealed to encode a cellular receptor responsible for binding anthrax toxin. Therefore, it is also referred to as Anthrax Toxin Recpetor 2, or *ANTXR2* (Scobie *et al.*, 2003). ANTXR2/CMG2 is one of two receptors known to bind anthrax toxin, the other being ANTXR1 (Bradley *et al.*, 2001), which is encoded by a gene originally referred to as Tumor Endothelial Marker 8 (*TEM8*), based on expression in tumor endothelium (St Croix *et al.*, 2000).

The significance of anthrax toxin binding in relation to endogenous receptor activity for ANTXR2/CMG2 remains unknown due to the fact that endogenous receptor function is not defined. However, there is growing evidence to support the idea that *ANTXR2/CMG2* may be a gene whose protein product regulates angiogenesis. As mentioned earlier, *ANTXR2/CMG2* was identified as a gene with dramatically up-regulated expression in cultured HUVEC induced to undergo capillary morphogenesis (Bell *et. al.*, 2001). Furthermore, extracellular matrix proteins such as type IV collagen and laminin may be endogenous ligands for the receptor (Bell *et al.*, 2001). Both of these extracellular proteins are components of vessel basement membranes and type IV collagen is critical for capillary formation *in vitro* (Bell *et al.*, 2001). Thus, interaction between ANTXR2/CMG2 and its native ligands may be important during angiogenic events. In addition, ANTXR2/CMG2 is closely related to the other anthrax toxin receptor, ANTXR1/TEM8. TEM8 splice variant 1 and $CMG2^{489}$ share 40% amino acid identity throughout their sequence and 60% identity within their vWF domains (Scobie *et al.*, 2003). Studies in support of an angiogenic function for ANTXR1/TEM8 have recently been published (Carson-Walter *et al.*, 2001; Hotchkiss *et al.*, 2005; Nanda *et al.*, 2004; Rmali *et al.*, 2005; St Croix *et al.*, 2000). Briefly, *ANTXR1/TEM8* has been identified as a gene specifically upregulated in tumor versus normal endothelium (St Croix *et al.*, 2000). Furthermore, *in vitro* assays have been used to establish that ANTXR1/TEM8 expression is important for endothelial migration on type I collagen matrices (Hotchkiss *et al.*, 2005) and tubule formation on matrigel (Rmali *et al.*, 2005).

Taken together, the data described above indicate that both ANTXR2/CMG2 and ANTXR1/TEM8 may be involved in physiological and pathological angiogenesis. As ANTXR2/CMG2 is expressed at higher levels in murine tissues than ANTXR1/TEM8 (Xu *et al.*, 2007) and has higher binding affinity for anthrax toxin (Scobie *et al.*, 2005), we have chosen to focus on the potential function of ANTXR2/CMG2 in angiogenesis and the endothelium. To test the hypothesis that ANTXR2/CMG2 is an angiogenic regulator, we performed an immunohistochemical survey of ANTXR2/CMG2 expression in a variety of normal mouse tissues and normal and malignant human breast tissues. We also assessed cellular function of ANTXR2/CMG2 *in vitro*. We establish that ANTXR2/CMG2 is expressed on murine and human vasculature *in vivo* and that ANTXR2/CMG2 is an angiogenic regulator critical for endothelial proliferation and capillary morphogenesis.

Materials and Methods

DNA constructs and cell lines

Anthrax toxin receptor deficient CHO-R1 cells engineered to express recombinant receptor-EGFP fusion proteins, $CMG2^{489}$-EGFP or ATR/TEM8sv2-EGFP, have been described (Scobie *et al.*, 2003). $CMG2^{489}$-EGFP fusion protein was engineered into retroviral vector pHyTCX. Human umbilical venous endothelial cells (HUVEC) were isolated from human umbilical vein as previously described (Jaffe *et al*., 1973) and cultured in EGM2 Bullet kit medium (Lonza, Basel, Switzerland) on dishes coated with type I rat tail collagen (VWR, West Chester, PA).

Cell Surface Receptor Expression Analysis

Flow cytometry analysis of ANTXR2/CMG2 and ANTXR1/TEM8 expression on the surface of transfected CHO cells has been previously described (Scobie *et al.*, 2006).

Animals

This study was conducted according to the National Institutes of Health *Guide for the Care and Use of Laboratory Animals*. Animal protocols were approved by the Institutional Animal Care and Use Committees. For all of the experiments, we used 6-week old female wild-type mice in the C57BL/6 background. After the mice were euthanized, the lungs were removed and insufflated with 2ml 10% neutrally buffered formalin. Colon samples and skin biopsies were surgically removed and fixed in 10% neutrally buffered formalin for 24 h, after which the samples were placed in 70% ethanol until processing. The tissue samples were paraffin embedded and 5 micron thick sections were cut and placed on Super-Frost Plus slides (Fisher, Waltham, MA) for immunohistochemistry.

Colormetric IHC

5 micron serial paraffin sections were deparaffinized in xylene, hydrated through a graded series of ethanol washes and placed in PBS. Antigen retrieval was performed by heating for 20 min in antigen retrieval solution (Dako, Carpinteria, CA). Endogenous peroxide activity was quenched by incubation in 3% hydgrogen peroxide/methanol solution for 10 min. Endogenous biotin was blocked using the Avidin/Biotin blocking kit (Vector Laboratories, Burlingame, CA). Prior to primary antibody application, tissue sections were blocked in phosphate-buffered saline (PBS) containing 3% bovine serum albumin and 2% normal serum (Sigma, St. Louis, MO) matching to the secondary antibody. Primary antibodies were incubated for one hour at room temperature. Primary antibodies used were chicken anti-human CMG2 (Scobie *et al.*, 2006) and rat anti-mouse CD31 (BD Pharmingen, San Jose, CA). Negative controls were left with blocking solution. Incubation with biotinylated secondary antibodies (Vector Laboratories, Burlingame, CA), specific to each primary antibody was performed for 30 min at room temperature and followed by incubation with avidin and horseradish-peroxidase conjugated biotin in PBS (Vectastain Standard ABC Elite kit, Vector Laboratories, Burlingame, CA). The color reaction was performed using DAB (diaminobenzidine tetrahydrochloride), the peroxidase substrate (Vector Laboratories, Burlingame, CA). Tissues were counterstained with hematoxylin (Fisher, Waltham, MA).

Studies utilizing human breast tissues were approved by Columbia University Institutional Review Board. 5 micron serial sections of frozen human breast tissue were fixed in cold acetone before immunostaining. Prior to primary antibody incubation, tissues were blocked as indicated above. Primary antibodies used were chicken anti-human CMG2 (Scobie *et al.*, 2006), mouse anti-human type IV collagen (Calbiochem) and mouse anti-human CD31 (Dako). Secondary antibody incubation and color reaction performed as indicated above.

Blocking experiments were performed by pre-incubating the chicken anti-human CMG2 antibody with 10-fold molar excess recombinant human CMG2 protein (Novus Biologicals, Littleton, CO) for two hours at room temperature before adding the antibody to slides. Images were obtained on Nikon ECLIPSE E 800 microscope (Nikon Inc., Melville, NY).

Immunofluorescent IHC

Immunostaining was performed as described above until application of secondary antibodies. Primary antibodies used were chicken anti-human CMG2 (Scobie *et al.*, 2006), rabbit anti-keratin K14 (Covance, Denver, PA a gift from Dr. David Owens, Columbia University), and rabbit anti-Involucrin (Li *et al.*, 2000), a gift from Dr. David Owens, Columbia University). Sections were incubated with biotinylated Alexa Fluor tagged secondary antibodies (Molecular Probes, Invitrogen, Carlsbad, CA), which were specific to each primary antibody. DAPI (4, 6-diamidino-2-phenylindole) (Sigma, St. Louis, MO) was used to visualize nuclei.

ANTXR2/CMG2 Gene Silencing

Three different CMG2 siRNA oligos were purchased from Ambion (Austin, TX) and screened via transient transfection and RT-PCR for adequate silencing of the *ANTXR2/CMG2* gene. The sequence resulting in knockdown of ANTXR2/CMG2 transcripts was used to generate oligos that were cloned into pSIREN retroviral vector (BD Biosciences, San Jose, CA) following manufacturer instructions. The siRNA target sense sequence was 5′ GCTAGCGAATGAACAAATTCA 3′. The resulting pSIREN-shCMG2 plasmid was used to generate retroviral cell lines as described below. Successful silencing of the *ANTXR2/CMG2* gene was confirmed by real time PCR as described below. pSIREN empty vector and pSIREN-scrambled shRNA were used as controls.

Gene Transfer into HUVEC

For retroviral gene transfer, the retroviral vector pSIREN or pHyTCX was used. GP293 packaging cells, 5×10^6 (Clontech, Mountain View, CA), were seeded and transfected with 10μg pSIREN-empty vector, scrambled shRNA, CMG2 shRNA, pHyTCX or pHyTC-CMG2^{489}GFP and 10μg pVSVG. Retroviral-containing supernatants were collected 48 h later, filtered and added to low passage HUVEC. 48 h after infection, pSIREN cell lines were selected for 5 days with puromycin (Invitrogen, Carlsbad, CA) at 3μg/ml and then maintained at 1.5μg/ml. pHyTCX infected cells were selected for 5 days with 300μg/ml hygromycinB (Invitrogen, Carlsbad, CA). *ANTXR2/CMG2* gene silencing and overexpression was confirmed via real time PCR as described below.

Quantitative RT-PCR Analysis

Total RNA was isolated using RNeasy kit (Qiagen, Valencia, CA) and first strand synthesis performed using random hexamers and Superscript II reverse transcriptase (Invitrogen, Carlsbad, CA). Quantitative real time PCR for β-actin, human CMG2 and mouse CMG2 (SYBER green PCR Master Mix, 7300 Real Time PCR system; Applied Biosystems, Foster City, CA) was performed in triplicate and values normalized for β-actin. Values are shown as fold difference compared to control. Real time PCR primers were as follows: mouse ANTXR2 exon1 Forward 5′-CTCTTGCAAAAAAGCCTTCG-3′ and Reverse 5′-TTCTTTGCCTCGTTCTCTGC-3′; mouse β-actin Forward 5′-CGAGGCCCAGAGCAAGAGAG-3′ and Reverse 5′-CTCGTAGATGGGCACAGTGTG-3′.

Indirect Immunocytochemistry

Cells seeded on type I collagen coated coverslips were washed with PBS, fixed with 4% paraformaldehyde, permeabilized with 0.1% Triton X-100, and blocked with PBS containing 3% BSA and 2% serum. Cells were incubated with chicken anti-CMG2 antibody followed by incubation with Alexa Fluor 594–coupled secondary antibody (Invitrogen). Controlcultures were incubated with secondary antibody alone. Coverslips were mounted with medium containing DAPI (4′6 diamidino-2-phenylindole; Vectashield; Vector Laboratories, Inc., Burlingame, CA). Cells were visualizedon Nikon ECLIPSE E 800 microscope.

Proliferation Assays In Vitro

Low-passage HUVEC were infected with retrovirus, as described above. pSIREN-empty vector and pSIREN-shCMG2 cells were seeded at 10,000 cells/well in serum free medium (SFM) supplemented with 20ng/ml EGF (Invitrogen, Carlsbad, CA) and 20ng/ml VEGF-A165 (Research Diagnostics, Inc., Concord, MA) on collagen-coated 24-well plates. Cell numbers were assessed 4 hours after seeding and at day 4 with the Cell Counting Kit-8 assay (Dojindo Molecular Technologies, Gaithersburg, MD) by preparing a calibration curve from known cell numbers, according to the manufacturer's instructions. All assays were performed in triplicate and repeated at least three times with three different cell lines.

Cell Cycle Analysis

Cells (10^5) were plated on type I collagen coated plates and cultured in complete medium. Four days later, cells were trypsinized and counted. 3×10^5 cells were pelleted, washed once in PBS and resuspended in .5ml cell cycle staining solution (50mg Propidium Iodide [Sigma Aldrich, St. Louis, MO], 1g NaCitrate [Fisher] in 1000ml distilled water). Cells were incubated 30 minutes at room temperature in the dark and maintained at 4°C before flow cytometry analysis on FACS Calibur (BD Bioscience). Living cells were gated according to propidium iodide staining. Data were analyzed via CellQuest Software (Beckton Dickinson). Six different control and knockdown cell lines were tested.

Capillary-like Network Formation Assay

Assays were performed as previously described (Tung *et al.*, 2009) All of the experiments were performed in triplicate and repeated at least three times with three different cell lines.

3D Tube Formation Assay

Porcine collagen gel (Wako USA, Richmond, VA) was prepared according to manufacturer's instructions. Retrovirally infected HUVEC were resuspended in collagen gel at 1×10^6 cells per 1 ml collagen gel and the cell/gel mixture was aliquoted 100ul per well into 24 well plates. The cell/gel suspension was allowed to polymerize at 37°C for 30 min. The cells were then cultured in SFM containing 40ng/ml EGF (Invitrogen, Carlsbad, CA), 40ng/ml bFGF (Invitrogen, Carlsbad, CA), and 40ng/ml VEGF-A165 (Research Diagnostics Inc., Concord, MA). The cultures were photographed after 72h. All of the experiments were performed in triplicate and repeated at least three times with three different cell lines.

Cell Migration Assays

For cellular-wound assays, retrovirally infected HUVEC were seeded to confluence on 24 well plates coated with type I collagen. 24 h later the cell monolayer was stripped away with a pipet tip across the diameter of each well. The medium and dislodged cells were aspirated and washed with PBS. Complete medium was added to the plates and cells were incubated at 37°C. Migration into the stripped areas was photographed at 0h and 12h time points. Visual assessment of the leading edge was made and marked accordingly for each time point. All of the experiments were performed in triplicate and repeated at least three times with three different cell lines.

For random cell movement assays, cells were sparsely plated (5×10^3) onto type I collagen (BD Biosciences) coated 4-well slides and allowed to adhere for 1 hour. Slides were then placed on a heated stage (37°C) and nuclear positions were tracked from phase images captured every 20 minutes over 10 hours on a Nikon TE300 microscope at 10X magnification. Cells that remained in the field of vision throughout the 10 hours without dividing or dying were used for analysis. Metamorph imaging software (Molecular Devices) was used to determine the *x* and *y* coordinates for the nucleus of each tracked cell and these coordinates were measured in pixels from frame to frame to ascertain distance traveled between frames. Distance traveled between frames was then added to yield the total distance (in pixels) migrated by each cell during 10 hours. These values were used to determine the average cellular speed of all the eligible cells in a group. Data is presented as average distance traveled in microns per hour (.645um per pixel).

Statistical analysis

Statistical significance was evaluated using the unpaired Student's *t* test with *P* value less than .05 considered statistically significant.

Results

ANTXR2/CMG2 is expressed in endothelial cells of murine skin, colon, lung and human breast tissue

ANTXR2/CMG2 expression has been documented at the transcript level in a variety of human tissues (Hanks *et al.*, 2003; Scobie *et al.*, 2003) however, careful assessment of ANTXR2/CMG2 expression by immunohistochemistry has not been reported. Previous studies suggest, but do not document, that ANTXR2/CMG2 is expressed on mammalian blood vessels. For instance, it has been reported that cultured HUVEC express endogenous ANTXR2/CMG2 (Bell *et al.*, 2001). To characterize the tissue specific and cellular distribution of ANTXR2/CMG2, we performed immunohistochemistry on a variety of normal mouse tissues using a chicken anti-CMG2 antibody that was raised against amino acids 1-232 of the human ANTXR2/CMG2 protein. We predicted that the antibody would detect ANTXR2/CMG2 in the mouse tissues analyzed as human and mouse ANTXR2/CMG2 are 93% identical at the amino acid level within the region recognized by the antibody. This antibody is specific for ANTXR2/CMG2 and does not detect the related ANTXR1/TEM8 protein (Scobie *et al.*, 2006). A control experiment, performed with the batch of antibody used in the present study, confirmed that it bound to ANTXR2/CMG2, and not to ANTXR1/TEM8, when these proteins were expressed on the surfaces of anthrax toxin receptor-deficient CHO-R1.1 cells (Figure 1a).

We proceeded to characterize ANTXR2/CMG2 expression in tissues that represent the main routes of entry for anthrax toxin into the body: skin, lung and intestine (Mock and Mignot, 2003). Immunofluorescence on mouse skin revealed that ANTXR2/CMG2 is expressed in the keratinocytes of the epidermis, in the outer root sheath of telogen hair follicles, on smooth muscle cells, and in the vascular endothelium (Figure 1b, 1c, 1d, 1g). ANTXR2/CMG2 expression in the epidermis was also confirmed at the transcript level via RT-PCR using cDNA from mouse primary keratinocytes (data not shown). As the epidermis is composed of proliferative and differentiated cell layers, we wanted to determine if ANTXR2/CMG2 is expressed throughout all epidermal layers or if expression is restricted to a particular layer(s). Therefore, the keratinocyte markers keratin K14 (proliferative) and involucrin (differentiated) were used in combination with ANTXR2/CMG2 to immunostain mouse skin. As expected, keratin K14 expression was detected in the basal layer of the epidermis and in the hair follicle outer root sheath (Figure 1e) and involucrin was localized to the suprabasal layers of the epidermis (Figure 1h). Co-staining mouse skin with ANTXR2/CMG2 and either keratin K14 or involucrin established that ANTXR2/CMG2 localizes with both of the keratinocyte markers (Figure 1f & 1i). Therefore, ANTXR2/CMG2 expression is not restricted to a particular layer of the epidermis, but seems to be expressed in all compartments. Immunostaining of mouse lung revealed that ANTXR2/CMG2 is highly expressed in the epithelial cells lining the aveoli, in the ciliated epithelial cells coating the bronchi, and in the vascular endothelium (Figure 2a). Similarly, immunostaining of the colon revealed that ANTXR2/CMG2 is highly expressed in the epilthelial cells lining the villi and on the vascular endothelium (Figure 2c & 2e). In order to confirm that ANTXR2/CMG2 is expressed on the vessels in these tissues, we compared ANTXR2/CMG2 expression to that of CD-31, an endothelial marker (Figure 2b, 2d, 2f). For

all of the tissues stained, we observed no detectable signal when using secondary antibody alone (data not shown). We also performed blocking studies to confirm antibody specificity. The chicken anti-human CMG2 antibody was pre-incubated with 10-fold molar excess of purified recombinant human ANTXR2/CMG2 protein and then used to immunostain mouse lung, colon and human skin. The immunostaining signal was greatly reduced in the epithelial cells lining the villi of mouse colon and the bronchioles of mouse lung as compared to unblocked antibody staining (Figure 2g, 2h, Supplemental Figure 1). In addition, the highly positive signal on the epidermis of the skin and on the blood vessels from all of the tissues analyzed was lost under blocking conditions (Figure 2h blow-up and Supplemental Figures 1a, 1b, 2a, 2b). We conclude that ANTXR2/CMG2 is expressed in a variety of cell types in lung, intestine and skin and definitive expression on endothelial cells was detected in each of these tissues.

The vasculature in the adult mouse tissues evaluated above is composed of quiescent endothelium. In order to determine if ANTXR2/CMG2 is expressed on angiogenic vessels, we next compared normal (quiescent) and malignant (angiogenic) human breast tissue. Fresh frozen serial sections of normal human mammary tissue obtained from reduction mammoplasties were subjected to immunohistochemical staining with anti-CMG2, anti-type IV collagen and anti-CD31 antibodies (Figure 3a, 3b, 3c respectively). ANTXR2/CMG2 expression was not detected in normal breast epithelium. However, the blood vessels (identified by CD31 staining) and basement membranes surrounding mammary ducts were clearly positive for ANTXR2/CMG2 (Figure 3a). Moreover, the ANTXR2/CMG2 expression pattern was identical to that of type IV collagen, a predicted ligand for CMG2 (Figure 3b). Type IV collagen is a known component of basement membranes.

Immunostaining serial sections of human breast cancer revealed that ANTXR2/CMG2 expression was localized to tumor basement membranes, tumor stroma and microvessels throughout both the tumor and stroma, but was absent from the tumor cells (Figure 3d). The ANTXR2/CMG2 expression pattern matched that seen for type IV collagen (Figure 3e) on vessel and tumor basement membranes. Furthermore, the ANTXR2/CMG2 staining pattern was lost in the presence of blocking peptide, confirming specificity of the antibody (Supplemental Figure 2c & 2d). Thus, in human tissue, CMG2 was found to be expressed on both quiescent and angiogenic vasculature and was found to colocalize with its ligand, type IV collagen.

ANTXR2/CMG2 expression is necessary for endothelial cell proliferation

The consistent expression of ANTXR2/CMG2 on endothelial cells of mouse and human tissues supports the hypothesis that it may be important in angiogenesis or endothelial cell function. To further explore this potential function, we utilized a series of *in vitro* angiogenesis assays with HUVEC to define the role of ANTXR2/CMG2 during distinct steps of angiogenic progression. To assess function, ANTXR2/CMG2 expression was reduced in HUVEC utilizing CMG2-specific RNAi expressed via retroviral vectors.

Retrovirally infected and puromycin selected HUVEC lines were generated to express empty vector (HUVEC/control), scrambled shRNA or shRNA targeting ANTXR2/CMG2 transcripts (HUVEC/shCMG2). Similar results were obtained when using either empty

vector or scrambled shRNA as the control cell line in a given experiment. The resulting cell lines were fixed and immunostained with chicken anti-human CMG2 antibody in order to evaluate ANTXR2/CMG2 protein levels. HUVEC/shCMG2 displayed reduced ANTXR2/CMG2 expression at the protein level as compared to empty vector control (Figure 4a). In addition, we observed reduced ANTXR2/CMG2 expression at the cell surface when the HUVEC lines were analyzed via flow cytometry with the ANTXR2/CMG2 antibody (Supplemental Figure 3a). ANTXR2/CMG2 knockdown was evaluated at the transcript level via real time PCR. We found that retroviral-delivered shRNA efficiently suppressed ANTXR2/CMG2 transcript expression in the HUVEC/shCMG2 lines from 30–85% as compared to control cell lines (Figure 4b).

Once ANTXR2/CMG2 knockdown was confirmed, the retroviral lines were used to examine the effect of reduced ANTXR2/CMG2 expression on endothelial cell proliferation. Equivalent numbers of empty vector control (HUVEC/control) and ANTXR2/CMG2 knockdown cells (HUVEC/shCMG2) were seeded on type I collagen coated plates and cultured for four days in the presence of serum-free medium (SFM) supplemented with EGF and VEGF-A. Reduction of ANTXR2/CMG2 expression led to a corresponding reduction in proliferation when compared to empty vector control (Figure 4c). For example, a HUVEC/shCMG2 A line with 30% knockdown of ANTXR2/CMG2 at the transcript level had a 50% reduction in proliferation while a HUVEC/shCMG2 B line with 85% knockdown at the transcript level had a 70% reduction in proliferation. Thus, the pattern of reduction correlated with the level of transcript knockdown obtained for each cell line. Moreover, this effect was not due to differences in seeding efficiency between the two cell lines as determined by WST-8 readings 4 hours after seeding (Supplemental Figure 3b).

As an alternative measure of proliferation, we performed flow cytometry with propidium iodide stained cells to assess DNA content. The resulting histograms consisted of three cell populations: those in G_0/G_1 phase, S phase and G_2/M phase of the cell cycle. The histogram in figure 4d is data from one experiment in which 60% of scrambled control cells were in G_0/G_1 phase and 40% were in S and G_2/M phase versus ANTXR2/CMG2 knockdown cells, which had 74% of cells in G_0/G_1 phase and 25% of cells in S and G_2/M phase. This data is one representative from six different experiments with six different cell lines in which the control cell lines had a higher proportion of dividing cells than the knockdown cell lines. Thus, the proliferation defect for ANTXR2/CMG2 knockdown cells was confirmed by two different experimental means.

Reduced ANTXR2/CMG2 expression does not significantly affect endothelial cell migration

We next evaluated whether endothelial cell migration is affected upon reduced ANTXR2/CMG2 expression via a cellular-wounding assay. Confluent monolayers of the retroviral HUVEC lines were disrupted with a pipet tip and endothelial cell migration into the stripped area was monitored over a 12 hour time period. ANTXR2/CMG2 knockdown resulted in a slight decrease in the migration rates of HUVEC on type I collagen as compared to empty vector control (Figure 5a); however, the magnitude of reduced migration in separate assays varied from undetectable to modest reduction. We obtained similar results when the cell lines were plated on the CMG2 ligand, type IV collagen (data not shown).

As proliferation is involved in cells re-occupying the wound during the cellular-wounding assay, we also wanted to evaluate chemokinesis via a random cell movement assay. In this assay, cells were seeded on type I collagen-coated slide wells and the movement of individual cells was recorded via time-lapse imaging over 10 hours. The results from this assay demonstrated little change in the average rate of cell movement between control cells and ANTXR2/CMG2 knockdown cells (Figure 5b). The control HUVEC had a migration rate of 30.7 microns/hour versus 27.4 microns/hour for the ANTXR2/CMG2 knockdown HUVEC ($P > .2$). Taken together, the results from the cellular-wounding and random cell movement assays demonstrate that reduced ANTXR2/CMG2 expression does not significantly affect endothelial cell migration/movement.

ANTXR2/CMG2 expression is required for capillary-like network formation in vitro

Since *ANTXR2/CMG2* gene expression has been reported to be up-regulated during capillary morphogenesis *in vitro* (Bell *et al.*, 2001), we assessed the affect of ANTXR2/CMG2 knockdown on their ability to organize into capillary-like networks or form lumen containing tubes. To assess capillary-like network formation the retroviral cell lines were seeded between two layers of porcine collagen gel and cultured in SFM supplemented with EGF and VEGF-A. The cells were photographed on day 4 of culturing. As shown in Figure 6A, the control cells formed a fine network of capillary-like cords. In contrast, ANTXR2/CMG2 knockdown inhibited VEGF-A-mediated capillary-like network formation (Figure 6a). Quantification of the surface area covered by the networks demonstrated that the formation of capillary-like structures was reduced by 50% in the knockdown cell line as compared with control (Figure 6b). Given that the cord structures formed during this assay rarely contain identifiable lumens, we also evaluated the affect of ANTXR2/CMG2 knockdown in HUVEC induced to undergo capillary tube formation when the cells are embedded in an extracellular matrix composed of porcine collagen gel. In this assay, HUVEC cells arrange into lumen-containing capillary-like tubes (Bell *et al.*, 2001). We found that ANTXR2/CMG2 knockdown impaired HUVEC morphogenesis into such capillary-like tubes (Figure 6c). Taken together this data suggests that endogenous expression of ANTXR2/CMG2 is necessary to make fine networks of neovessels using HUVEC.

CMG2 overexpression increases endothelial cell proliferation and capillary-like network formation but not migration

To compliment the loss-of-function approach taken above, we generated stable cell lines overexpressing ANTXR2/CMG2. HUVEC lines were generated by transduction with retrovirus encoding no protein or $CMG2^{489}$ fused to GFP (HUVEC/CMG2GFP). Fluorescent microscopy was used to verify overexpression of ANTXR2/CMG2 by checking the GFP-based fluorescence associated with the recombinant receptor. While ANTXR2/CMG2 knockdown was found to decrease endothelial cell proliferation, overexpression of ANTXR2/CMG2 increased cellular proliferation by almost 40% (Figure 7a). As expected, cellular migration rates remained unchanged when ANTXR2/CMG2 was overexpressed (Figure 7b). This was consistent with the observation that ANTXR2/CMG2 knockdown did not significantly affect endothelial cell migration. ANTXR2/CMG2 overexpression did, however, increase the network of capillary-like cords formed in the sandwich network

formation assay (Figure 7c). Quantification of the surface area covered by the networks demonstrated that the formation of capillary-like structures was increased by approximately 50% upon ANTXR2/CMG2 overexpression as compared with control (Figure 7d).

Discussion

ANTXR2/CMG2 was originally identified as a gene with up-regulated expression during capillary morphogenesis suggesting a potential role in angiogenesis, however, little is known about its function. Here we report analysis of the potential angiogenic function of ANTXR2/CMG2 using two approaches. First, we establish that ANTXR2/CMG2 is expressed in blood vessels found in several tissues, including murine skin, lung and colon and normal and tumorigenic human breast tissue. Second, utilizing *in vitro* assays, we report that ANTXR2/CMG2 knockdown diminishes endothelial cell proliferation and the ability to form capillary-like structures while ANTXR2/CMG2 overexpression increases proliferation. We conclude that ANTXR2/CMG2 functions in endothelial cell proliferation and morphogenesis.

Angiogenic regulators are either widely expressed in many cell types or can be endothelial specific in their expression. The latter category includes proteins such as VEGFR-2 and VE-Cadherin, both of which are involved in angiogenesis and vascular integrity and these proteins primarily function in endothelial cells. The two anthrax receptor genes, *ANTXR2/CMG2* and *ANTXR1/TEM8*, were originally identified in endothelial cells (Bell *et al.*, 2001; St Croix *et al.*, 2000)and this suggested potential roles in angiogenesis. In the case of *ANTXR1/TEM8,* original reports of tumor endothelial-specific expression have been supplemented with studies documenting expression in several cell types, including but not limited to endothelium (Bonuccelli *et al.*, 2005; Carson-Walter *et al.*, 2001; Nanda *et al.*, 2004). Little was known regarding ANTXR2/CMG2 protein expression and thus we performed an immunohistochemical survey of mouse lung, colon and skin tissues and normal and tumorigenic human breast tissue. We report that ANTXR2/CMG2 is widely expressed in a variety of cell types including quiescent and angiogenic endothelial cells (Figures 1, 2 & 3). Using histological analysis and staining with cell-specific markers, we show ANTXR2/CMG2 expression in blood vessels of skin (Figure 1), colon (Figure 2), and lung (Figure 2). In dermis, strong expression was found on keratinocytes, which were identified both histologically and based upon expression of keratin K14 and involucrin. In addition, we detected ANTXR2/CMG2 transcripts expressed in cultured keratinocytes (data not shown). In colon and lung, ANTXR2/CMG2 was also expressed in epithelial cells.

It is possible that the ANTXR2/CMG2 expression pattern detected in mouse tissues could reflect the combined expression pattern of ANTXR2/CMG2 and ANTXR1/TEM8, as our data and a previously published report (Bonuccelli *et al.*, 2005) indicate that the two proteins are expressed in many of the same cell types. The peptide sequence used to raise the anti-human ANTXR2/CMG2 antibody shares approximately 52% identity with mouse ANTXR1/TEM8. However, ANTXR2/CMG2 transcripts have been detected in all three of the mouse tissues we analyzed and it has been reported that the ratios of ANTXR2/CMG2 to ANTXR1/TEM8 mRNA expression levels are 20:1 in the gastrointestinal tract and 4:1 in both the lung and skin (Xu *et al.*, 2007), indicating that ANTXR2/CMG2 may be the major anthrax toxin receptor expressed. The immunohistochemical analysis performed on normal

mouse tissues likely represents the expression pattern of ANTXR2/CMG2 when one considers the following: i) blocking studies using a human ANTXR2/CMG2 blocking peptide reduced the signal in the mouse tissues; and ii) the location of ANTXR2/CMG2 expression in mouse skin directly parallels its location in human skin, where cross-reactivity with human ANTXR1/TEM8 does not occur.

It had been previously reported that ANTXR1/TEM8 expression is specific to tumor endothelium as its expression was absent from quiescent endothelium in normal adult tissues (Nanda and St Croix, 2004). This is not the case for ANTXR2/CMG2. Analysis of normal and malignant human breast tissue revealed that ANTXR2/CMG2 was expressed on both quiescent and angiogenic vessels (Figure 3). In normal breast, ANTXR2/CMG2 was found in vessels of the stroma and in the basement membrane surrounding the epithelial ducts, however, expression was not seen in ductal epithelium. As in normal breast, basement membrane surrounding ductal carcinoma cells retained the ANTXR2/CMG2 expression. The tumor vessels that grew into the ductal carcinomas were clearly ANTXR2/CMG2 positive. Furthermore, the ANTXR2/CMG2 expression pattern colocalized with that of type IV collagen, a putative ANTXR2/CMG2 ligand, in both normal and malignant human breast tissue. This is the first study demonstrating receptor-ligand colocalization, suggesting that type IV collagen may in fact be an endogenous ligand for ANTXR2/CMG2.

Based upon our immunohistochemical analyses, we conclude that ANTXR2/CMG2 is expressed in endothelium, kertinocytes and a variety of other cell types. It is not known how ANTXR2/CMG2 may function in these diverse cell types but it is clear that ANTXR2/CMG2 is expressed in several cells that come in contact with *Bacillus anthracis*, the causative agent of anthrax.

Given the expression of ANTXR2/CMG2 in endothelium of mouse and human tissues, we next explored ANTXR2/CMG2 function in endothelial cells. We chose shRNA-mediated knockdown of ANTXR2/CMG2 expression as a means of inhibiting ANTXR2/CMG2 activity. Endothelial cells with reduced ANTXR2/CMG2 expression were generated using RNA interference. An ANTXR2/CMG2 siRNA-specific decrease in transcript and protein levels was confirmed by real time PCR and immunostaining of the retroviral cell lines (Figure 4). The most striking effect of this reduced expression was the significant decrease in endothelial proliferation we observed in HUVEC. This effect was not previously suggested from analysis of ANTXR1/TEM8 function (Hotchkiss *et al.*, 2005; Rmali *et al.*, 2005). ANTXR2/CMG2 knockdown also adversely affected the ability of endothelial cells to form capillary-like networks *in vitro*. This assay depends on proper angiogenic signals to stimulate endothelial cell morphogenesis and branching. As shown in Figure 6, reduced ANTXR2/CMG2 expression clearly disrupted capillary-like network and tube formation. As network formation is known to occur rapidly in these assays, we believe this is a direct effect on the ability of endothelial cells to form cords and tube-like structures. Finally, overexpression of ANTXR2/CMG2 was found to have the opposite affect of knockdown in that it promoted endothelial cell proliferation and network formation (Figure 7). Thus, primary endothelial cells depend on proper ANTXR2/CMG2 expression to undergo normal cell proliferation and capillary-like network formation - key steps in angiogenesis.

This is the first study to demonstrate that knockdown of ANTXR2/CMG2 expression strongly inhibits endothelial cell function *in vitro*. The mechanism by which ANTXR2/CMG2 promotes these processes remains to be determined. However, given ANTXR2/CMG2 protein structure and ligand binding capabilities, a likely mechanism involves modulating endothelial cell-extracellular matrix interactions. Additional support for this idea is provided by recently published data in which protective antigen (PA), the receptor-binding moiety of anthrax toxin, was used as a receptor antagonist. PA was demonstrated to inhibit endothelial cell function *in vitro* and angiogenesis *in vivo* by interfering with the binding of ANTXR2/CMG2 or ANTXR1/TEM8 to their endogenous ligands, extracellular matrix proteins (Rogers *et al.*, 2007). Furthermore, characterization of the protein domains responsible for contributing to ANTXR1/TEM8 function revealed that the von Willebrand factor type A (vWF) and the transmembrane domains, as opposed to the intracellular portion of the protein, might be the domains necessary for promoting ANTXR1/TEM8 angiogenic functions (Rmali *et al.*, 2005). The vWF domain is thought to be the ligand-binding domain on ANTXR1/TEM8, thus protein/ECM interactions are hypothesized to be integral to ANTXR1/TEM8 angiogenic function. Future work will determine if the same holds true for ANTXR2/CMG2.

While ANTXR2/CMG2 and ANTXR1/TEM8 are closely related, their endogenous functions in endothelial cells may be distinct from one another. Overexpression of ANTXR1/TEM8 has been demonstrated to promote endothelial cell migration but not proliferation or network formation (Hotchkiss *et al.*, 2005). Antagonizing ANTXR1/TEM8 function, via the use of a secreted ANTXR1/TEM8 extracellular domain or via knockdown with hammerhead ribozymes, inhibited endothelial cell migration and network formation (Hotchkiss *et al.*, 2005; Rmali *et al.*, 2005). In contrast, knockdown of ANTXR2/CMG2 resulted in strong inhibition of endothelial cell proliferation and network/tube formation while overexpression of ANTXR2/CMG2 promoted proliferation and network formation. Neither knockdown nor overexpression of ANTXR2/CMG2 had an effect on migration. As such, ANTXR1/TEM8 may function in endothelial cell migration whereas ANTXR2/CMG2 may function in proliferation and tube formation. If so, it will be interesting to explore how the two anthrax toxin receptors function in distinct endothelial cell behaviors. During preparation of this manuscript, an *Antxr2/Cmg2* knockout mouse was reported on and found to be viable, indicating that developmental angiogenesis was not impaired upon *Antxr2/Cmg2* deletion (Liu *et al.*, 2009), however postnatal and pathological angiogenesis was not evaluated in this study. In light of this report, it is possible that *Antxr1/Tem8* may compensate for lack of *Antxr2/Cmg2* function in the mouse. Therefore, it will be informative to generate mice deficient in both *Antxr1/Tem8* and *Antxr2/Cmg2*.

In conclusion, we have demonstrated that ANTXR2/CMG2 is expressed on the vasculature *in vivo* and that ANTXR2/CMG2 functions to promote angiogenic processes. Our study makes it increasingly evident that ANTXR2/CMG2 is an angiogenic regulator. Future studies will help define the physiological and pathological function of these receptors in vasculature. For instance, one can determine if tumor endothelium depends on proper activity of ANTXR2/CMG2 in order to rapidly grow into an avascular cancerous tissue.

Supplementary Material

Refer to Web version on PubMed Central for supplementary material.

Acknowledgments

Funding: This work was supported by NIH RO1 HL62454 (J.K.K.) and NIH RO1 AI064654 (J.K.K.). C.V.R. was supported by endocrinology training grant DK07328 and by a fellowship from the DOD Breast Cancer Program X81WH-06-1-0355. J.Y. was supported by NIH grant AI48489.

This work was supported by NIH RO1 HL62454 (J.K.K.) and NIH RO1 AI064654 (J.K.K.). C.V.R. was supported by endocrinology training grant DK07328 and by a fellowship from the DOD Breast Cancer Program X81WH-06-1-0355. J.Y. was supported by NIH grant AI48489. We thank Dr. Yasuhiro Funahashi, Ayelet Spitzer and Eunice Kim for technical support, Dr. David Owens for the gift of the antibodies and critical reading of the manuscript and Dr. Darrell Yamashiro for help with preparation of the figures.

Abbreviations

CMG2	Capillary Morphogenesis Gene 2
ANTXR2	Anthrax toxin receptor 2
HUVEC	human umbilical venous endothelial cell
EC	endothelial cell
VEGF	vascular endothelial growth factor
EGF	epidermal growth factor
ANTXR1	Anthrax toxin receptor 1
TEM8	Tumor Endothelial Marker 8
SFM	serum free medium
shRNA	short hairpin RNA
PA	protective antigen

References

Adams RH, Alitalo K. Molecular regulation of angiogenesis and lymphangiogenesis. Nat Rev Mol Cell Biol. 2007; 8:464–78. [PubMed: 17522591]

Armulik A, Abramsson A, Betsholtz C. Endothelial/pericyte interactions. Circ Res. 2005; 97:512–23. [PubMed: 16166562]

Bell SE, Mavila A, Salazar R, Bayless KJ, Kanagala S, Maxwell SA, et al. Differential gene expression during capillary morphogenesis in 3D collagen matrices: regulated expression of genes involved in basement membrane matrix assembly, cell cycle progression, cellular differentiation and G-protein signaling. J Cell Sci. 2001; 114:2755–73. [PubMed: 11683410]

Bonuccelli G, Sotgia F, Frank PG, Williams TM, de Almeida CJ, Tanowitz HB, et al. ATR/TEM8 is highly expressed in epithelial cells lining Bacillus anthracis' three sites of entry: implications for the pathogenesis of anthrax infection. Am J Physiol Cell Physiol. 2005; 288:C1402–10. [PubMed: 15689409]

Bradley KA, Mogridge J, Mourez M, Collier RJ, Young JA. Identification of the cellular receptor for anthrax toxin. Nature. 2001; 414:225–9. [PubMed: 11700562]

Carmeliet P, Jain RK. Angiogenesis in cancer and other diseases. Nature. 2000; 407:249–57. [PubMed: 11001068]

Carson-Walter EB, Watkins DN, Nanda A, Vogelstein B, Kinzler KW, St Croix B. Cell surface tumor endothelial markers are conserved in mice and humans. Cancer Res. 2001; 61:6649–55. [PubMed: 11559528]

Hanks S, Adams S, Douglas J, Arbour L, Atherton DJ, Balci S, et al. Mutations in the gene encoding capillary morphogenesis protein 2 cause juvenile hyaline fibromatosis and infantile systemic hyalinosis. Am J Hum Genet. 2003; 73:791–800. [PubMed: 14508707]

Hotchkiss KA, Basile CM, Spring SC, Bonuccelli G, Lisanti MP, Terman BI. TEM8 expression stimulates endothelial cell adhesion and migration by regulating cell-matrix interactions on collagen. Exp Cell Res. 2005; 305:133–44. [PubMed: 15777794]

Jaffe EA, Nachman RL, Becker CG, Minick CR. Culture of human endothelial cells derived from umbilical veins. Identification by morphologic and immunologic criteria. J Clin Invest. 1973; 52:2745–56. [PubMed: 4355998]

Li ER, Owens DM, Djian P, Watt FM. Expression of involucrin in normal, hyperproliferative and neoplastic mouse keratinocytes. Exp Dermatol. 2000; 9:431–8. [PubMed: 11099111]

Liu S, Crown D, Miller-Randolph S, Moayeri M, Wang H, Hu H, et al. Capillary morphogenesis protein-2 is the major receptor mediating lethality of anthrax toxin in vivo. Proc Natl Acad Sci U S A. 2009; 106:12424–9. [PubMed: 19617532]

Mock M, Mignot T. Anthrax toxins and the host: a story of intimacy. Cell Microbiol. 2003; 5:15–23. [PubMed: 12542467]

Nanda A, Carson-Walter EB, Seaman S, Barber TD, Stampfl J, Singh S, et al. TEM8 interacts with the cleaved C5 domain of collagen alpha 3(VI). Cancer Res. 2004; 64:817–20. [PubMed: 14871805]

Nanda A, St Croix B. Tumor endothelial markers: new targets for cancer therapy. Curr Opin Oncol. 2004; 16:44–9. [PubMed: 14685092]

Risau W. Mechanisms of angiogenesis. Nature. 1997; 386:671–4. [PubMed: 9109485]

Rmali KA, Puntis MC, Jiang WG. TEM-8 and tubule formation in endothelial cells, its potential role of its vW/TM domains. Biochem Biophys Res Commun. 2005; 334:231–8. [PubMed: 15993844]

Rogers MS, Christensen KA, Birsner AE, Short SM, Wigelsworth DJ, Collier RJ, et al. Mutant anthrax toxin B moiety (protective antigen) inhibits angiogenesis and tumor growth. Cancer Res. 2007; 67:9980–5. [PubMed: 17942931]

Scobie HM, Rainey GJ, Bradley KA, Young JA. Human capillary morphogenesis protein 2 functions as an anthrax toxin receptor. Proc Natl Acad Sci U S A. 2003; 100:5170–4. [PubMed: 12700348]

Scobie HM, Thomas D, Marlett JM, Destito G, Wigelsworth DJ, Collier RJ, et al. A soluble receptor decoy protects rats against anthrax lethal toxin challenge. J Infect Dis. 2005; 192:1047–51. [PubMed: 16107958]

Scobie HM, Wigelsworth DJ, Marlett JM, Thomas D, Rainey GJ, Lacy DB, et al. Anthrax toxin receptor 2-dependent lethal toxin killing in vivo. PLoS Pathog. 2006; 2:e111. [PubMed: 17054395]

Shimaoka M, Lu C, Salas A, Xiao T, Takagi J, Springer TA. Stabilizing the integrin alpha M inserted domain in alternative conformations with a range of engineered disulfide bonds. Proc Natl Acad Sci U S A. 2002; 99:16737–41. [PubMed: 12466503]

St Croix B, Rago C, Velculescu V, Traverso G, Romans KE, Montgomery E, et al. Genes expressed in human tumor endothelium. Science. 2000; 289:1197–202. [PubMed: 10947988]

Tung JJ, Hobert O, Berryman M, Kitajewski J. Chloride intracellular channel 4 is involved in endothelial proliferation and morphogenesis in vitro. Angiogenesis. 2009

Xu Q, Hesek ED, Zeng M. Transcriptional stimulation of anthrax toxin receptors by anthrax edema toxin and Bacillus anthracis Sterne spore. Microb Pathog. 2007; 43:37–45. [PubMed: 17459655]

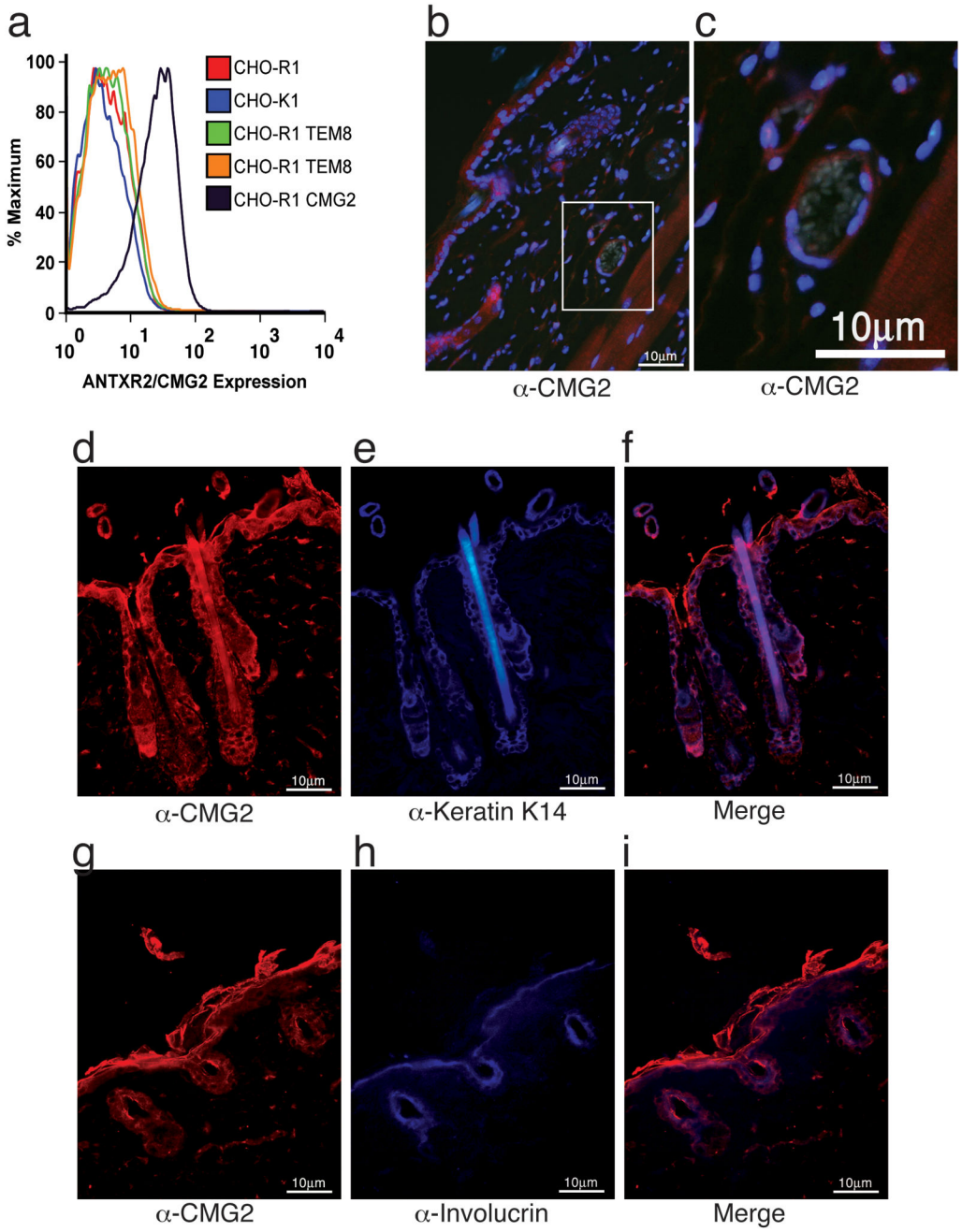

Figure 1. ANTXR2/CMG2 expression in normal mouse skin

(a) Detection of CMG2 on the cell surface by flow cytometry using the chick anti-human CMG2 antidbody. (b–i) Immunofluorescence. Thin sections (5μm) from formalin-fixed paraffin embedded mouse skin were stained with fluorescent conjugates. (b) ANTXR2/CMG2 in skin, red-ANTXR2/CMG2, blue-nuclei (DAPI). (c) Boxed area from b enlarged to highlight ANTXR2/CMG2 expression on blood vessels in the skin. (d–i) Double labeling: red-ANTXR2/CMG2 (d, g), blue-Keratin K14 (e) or Involucrin (h), purple-coexpression of ANTXR2/CMG2 with either Keratin K14 (f) or Involucrin (i). Images were taken at 40X magnification.

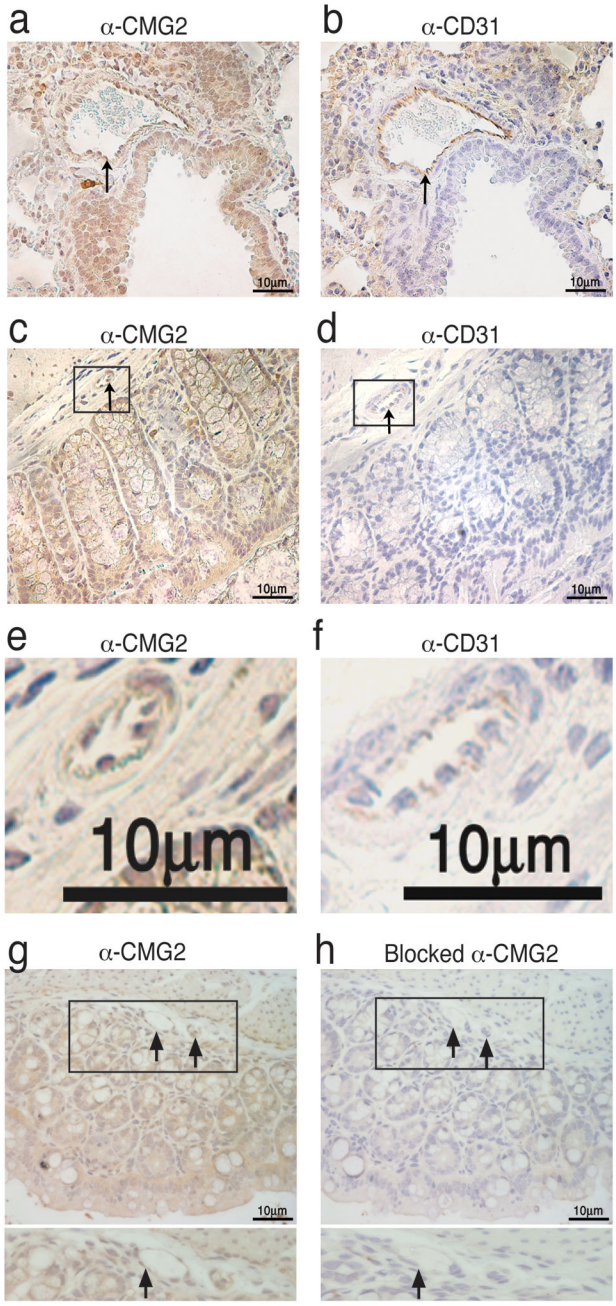

Figure 2. ANTXR2/CMG2 expression in normal mouse lung and colon

Colormetric immunohistochemisty on thin sections (5μm) from formalin-fixed paraffin embedded mouse lung and colon. (a) ANTXR2/CMG2 in lung. (b) CD31 in lung. (c) ANTXR2/CMG2 in colon. (d) CD31 in colon. (e & f) Boxed areas from c & d are enlarged to highlight vasculature in colon. Brown ANTXR2/CMG2 or CD31. Blue—nuclei (hematoxylin). (g) ANXTR2/CMG2 expression in colon with boxed area enlarged to highlight a positively stained vessel. (h) ANTXR2/CMG2 staining in colon is reduced after pre-incubation of the antibody with 10-fold molar excess recombinant CMG2 protein. Arrows indicate blood vessels in all of the tissues. Images were taken at 40X magnification.

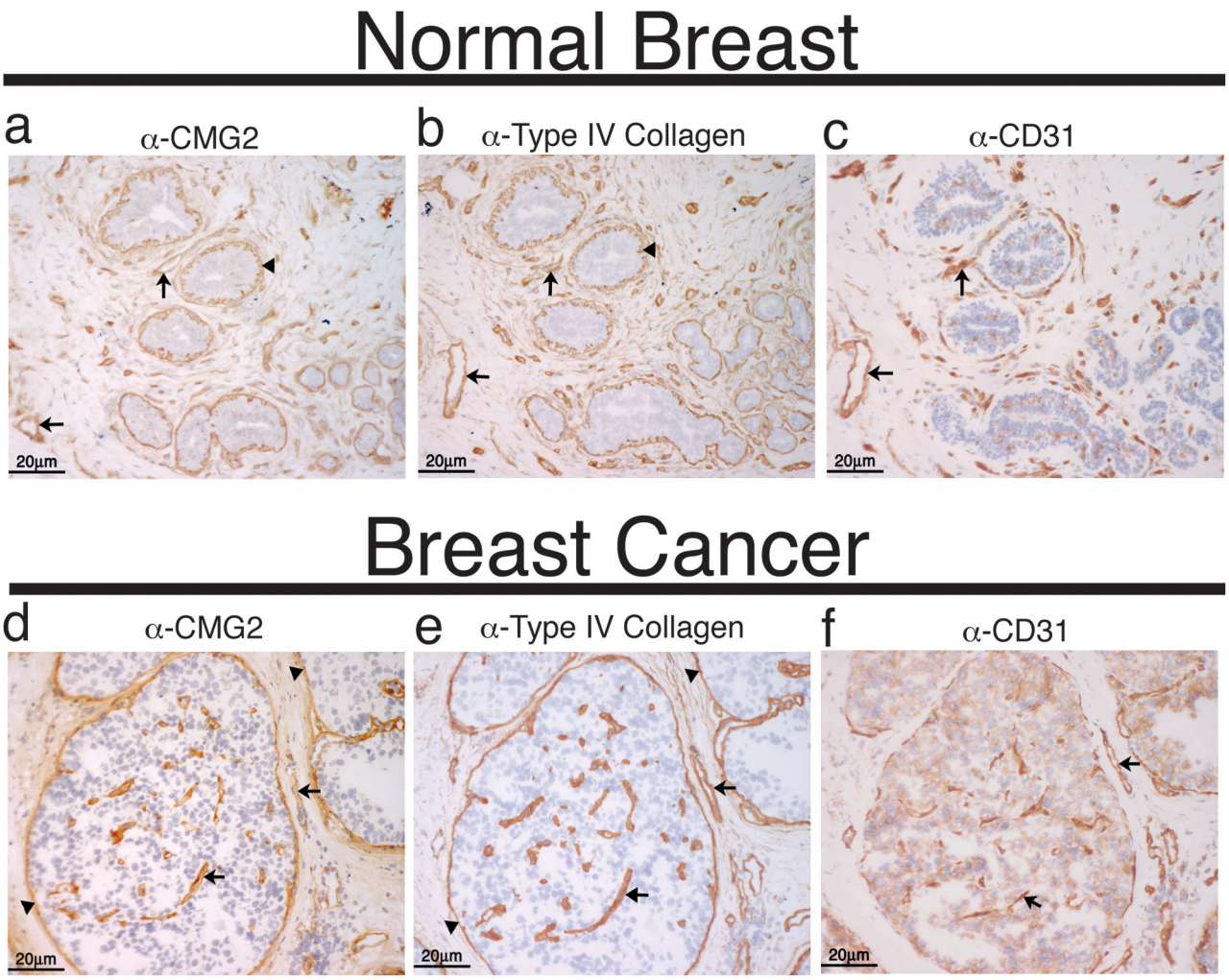

Figure 3. ANTXR2/CMG2 expression in normal and malignant human breast tissue

Colormetric immunohistochemistry on thin sections (5μm) from fresh frozen human breast tissue. (a–c) Serial sections of normal human mammary tissue. (d–f) Serial sections of human breast cancer. (a, d) ANTXR2/CMG2. (b, e) Type IV Collagen. (c, f) CD31. Counterstaining with hematoxylin. Arrows indicate blood vessels. Arrowheads indicate basement membranes surrounding mammary ducts or tumor. All images were taken at 20X magnification.

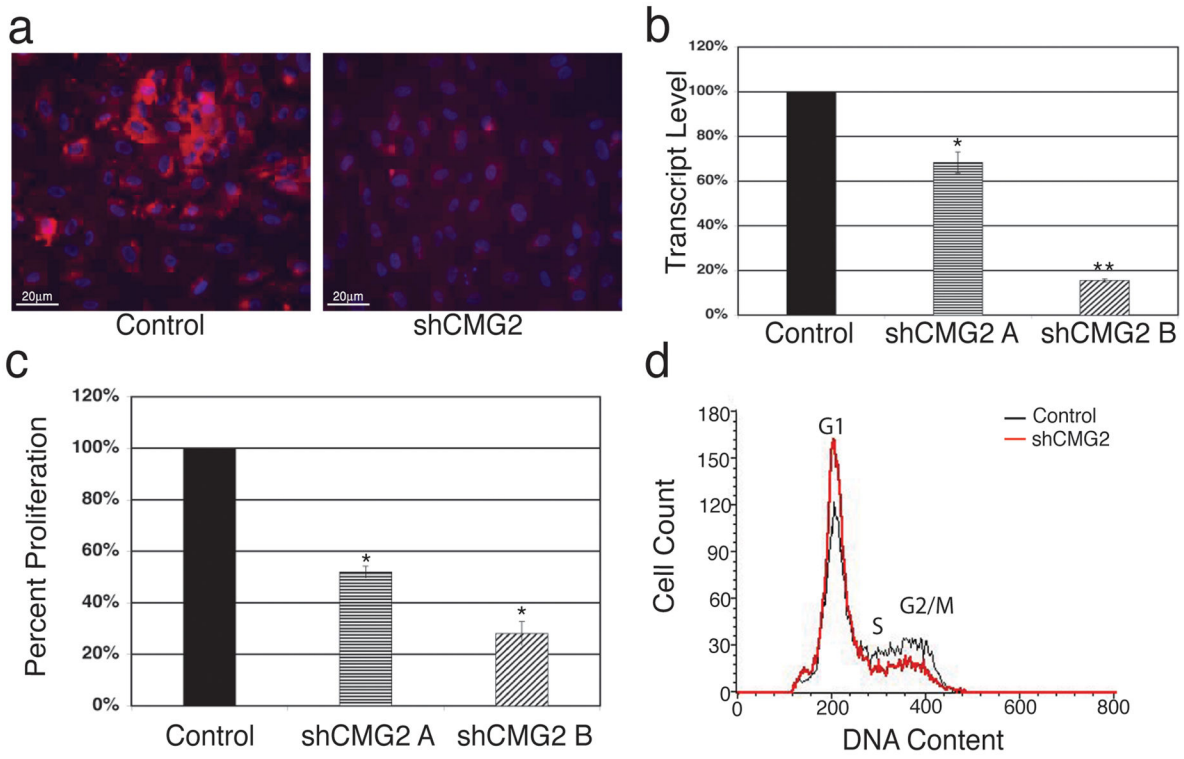

Figure 4. Knockdown of ANTXR2/CMG2 expression inhibits HUVEC proliferation

(a) Fluorescent microscopy images of retrovirally-infected HUVEC empty vector (control) or ANTXR2/CMG2 shRNA (shCMG2) cell lines immunostained with anti-CMG2 antibody; Red-ANTXR2/CMG2, Blue-nuclei (DAPI). 20X magnification. (b) Real time PCR analysis on total cDNA from HUVEC empty vector (control) or two different cell lines expressing shRNA specific for ANTXR2/CMG2 (shCMG2 A & shCMG2 B) to detect knockdown of gene expression. β-actin expression was used to normalize samples. The data is shown as percentage of control ± standard deviation and represents two independent experiments. (*$P < .01$, ** $P < .001$) (c) The HUVEC lines shown in panel b showed reduced cell growth after 4 days of culture as determined by WST-8 assay (see materials and methods). The percentage decrease in cell number was based upon corresponding controls. The data represents two independent experiments. (*$P < .001$) Error bars are the calculated standard deviation. (d) Flow cytometry analysis of cell cycle (propidium iodide) profiles of retroviral HUVEC cells lines expressing control or ANTXR2/CMG2 shRNA (shCMG2). Cell Quest software was used to assess cell cycle distribution. A representative experiment from six independent sets of experiments is shown.

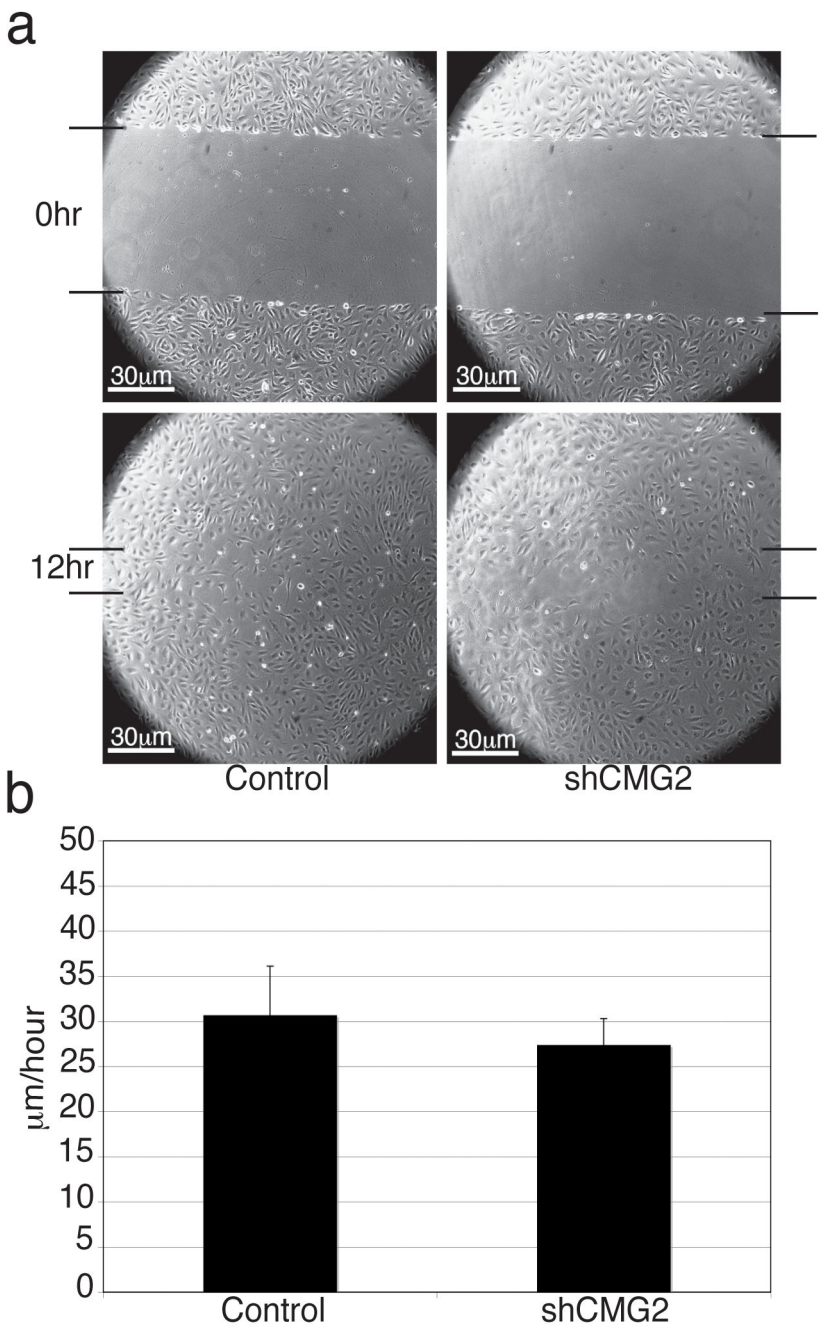

Figure 5. Knockdown of ANTXR2/CMG2 expression does not significantly affect HUVEC migration

(a) Representative images of a cellular-wound assay immediately (0hr) and 12 hours after wounding. Retroviral HUVEC lines expressing ANTXR2/CMG2 shRNA (shCMG2) showed a slight change in migration as measured 12 hours after wounding when compared with empty vector (control) cell lines. Images were taken at 10X magnification. Black bars indicate cell front. (b) A bar graph plotting the average movement rates in microns/hour of the retroviral HUVEC control and shCMG2 lines during random cell movement assays. Columns represent the average of three independent experiments; bars represent standard

deviation. No significant change ($P > .2$) in random cell movement was detected between the control and ANTXR2/CMG2 knockdown HUVEC as determined by an unpaired Student's *t*-test with a $P < .05$ being considered statistically significant.

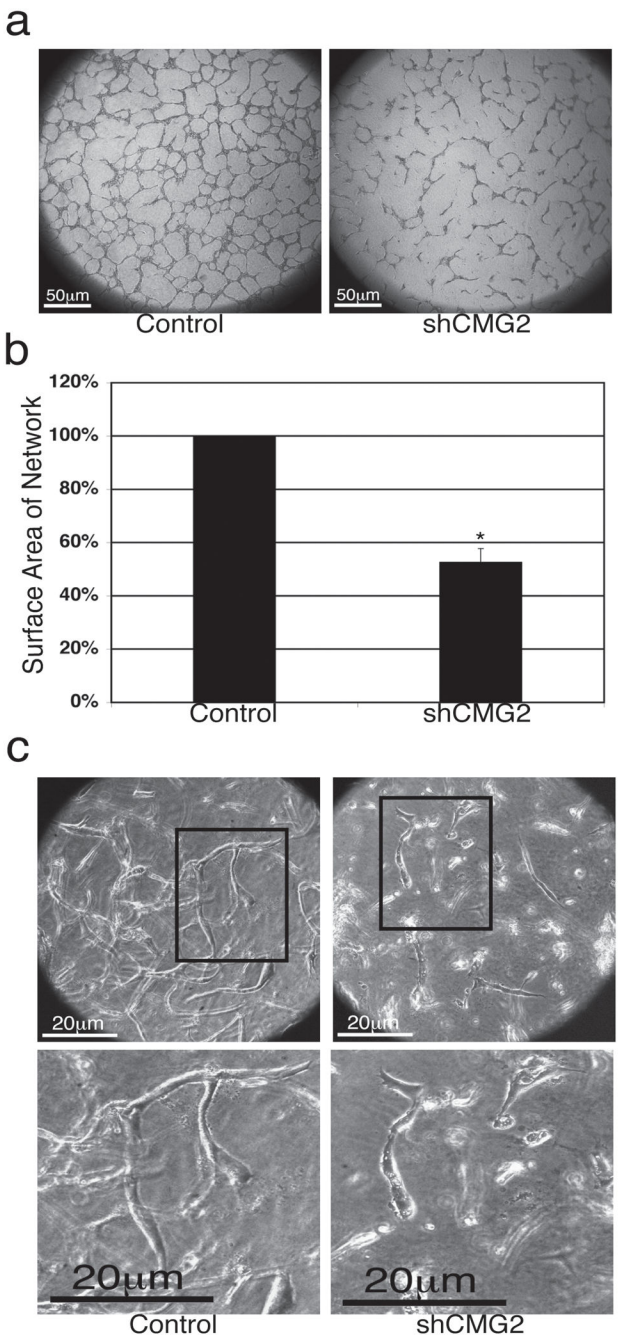

Figure 6. Knockdown of ANTXR2/CMG2 expression inhibits HUVEC network and tube formation

(a) Retroviral HUVEC lines expressing ANTXR2/CMG2 shRNA (shCMG2) showed reduced ability to form networks when compared with empty vector (control) HUVEC in the capillary-like network formation assay. Images were taken at 5X magnification. A representative experiment is shown. (b) Quantification of surface area covered by networks in control and shCMG2 HUVEC lines. Data is shown as percentage of control ± standard deviation. (*$P < .01$) (c) Retroviral HUVEC lines expressing ANTXR2/CMG2 shRNA (shCMG2) showed reduced ability to form tubes when compared with empty vector control

in a 3D tube formation assay. Top images were taken at 20X magnification. Boxed areas are enlarged to highlight tube structures. A representative experiment is shown.

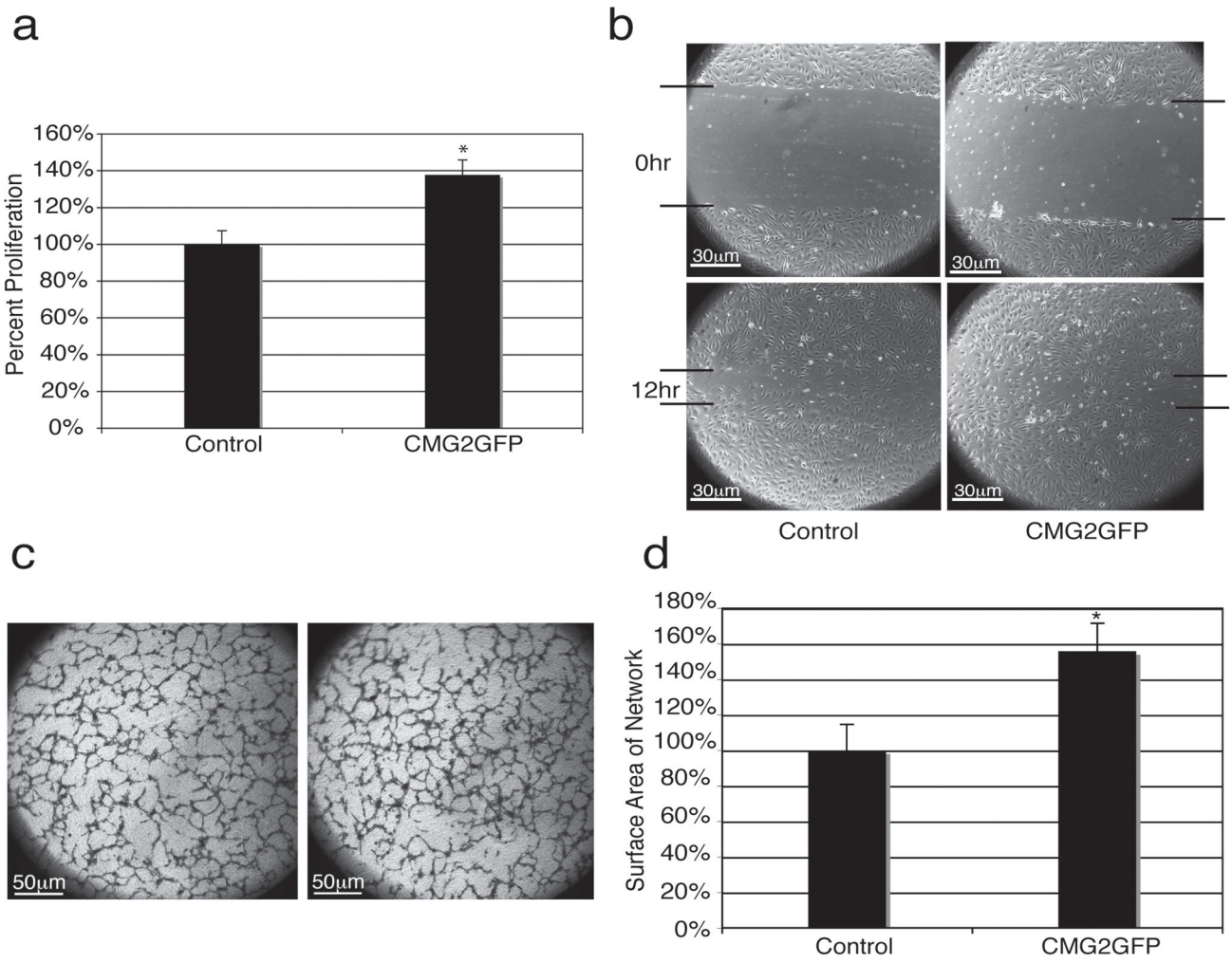

Figure 7. ANTXR2/CMG2 overexpression promotes HUVEC proliferation and capillary-like network formation but does not affect HUVEC migration

(a) Retroviral HUVEC cell lines overexpressing a CMG2GFP fusion protein (CMG2GFP) showed increased cell growth after 4 days of culture as determined by WST-8 assay (see materials and methods). The percentage increase in cell number was based upon corresponding empty vector controls. (* $P < .01$) A representative experiment from three independent experiments is shown. Error bars are the calculated standard deviation. (b) Images of a cellular-wound assay immediately (0hr) and 12 hours after wounding. Retroviral HUVEC lines overexpressing a CMG2GFP fusion protein (shCMG2) exhibited no change in migration rates as measured 12 hours after wounding when compared with empty vector (control) cell lines. Images were taken at 10X magnification. Black bars indicate cell front. Images are representative of three independent experiments. (c) Retroviral HUVEC lines overexpressing CMG2GFP showed increased ability to form networks when compared to control HUVEC in the capillary-like network formation assay. Images were taken at 5X magnification. A representative experiment from three independent experiments is shown.

(b) Quantification of surface area covered by networks in control and CMG2GFP HUVEC lines. (* $P < .001$) Data is shown as percentage of control ± standard deviation.